

BIOENERGETICS

Water route for proton pumping in mitochondrial complex I

A new cryo-EM structure of mitochondrial complex I reveals ordered water molecules that connect key elements of the proton-translocating machinery. Analysis of the ubiquinone-binding site of complex I offers insights into the mechanism of catalytic turnover and the regulation of this essential metabolic enzyme.

Alexander Galkin

Mitochondrial aerobic respiration is carried out by a number of membrane protein complexes that transfer electrons from substrates (NADH, succinate, glycerol 3-phosphate, and so on) to ubiquinone and then to molecular oxygen. In three of these enzymes (complexes I, III and IV), electron flow is coupled to the pumping of protons across the inner mitochondrial membrane, creating a proton gradient that drives ATP synthase. Our understanding of both the proton-pumping mechanism of complex I and the details of its physiological regulation has been hampered by the lack of structural information. The 2.7-Å-resolution structure of complex I from aerobic yeast *Yarrowia lipolytica* by Grba and Hirst¹ is the most accurate map of this mitochondrial enzyme to date. The structure reveals a number of ordered water molecules bound to key domains (Fig. 1): some supply protons to reduce ubiquinone, whereas others link critical elements of the proton-pumping machinery and probably participate directly in vectorial proton (\vec{H}^+) translocation.

Importantly, this study also allows detailed comparison between the active and deactive (A/D) complex I conformational states², as the transition between these states plays an essential role in the pathophysiology of the tissue response to ischemia^{3,4}. Overall, this study provides important new insights into mitochondrial complex I and will guide experimental and computational approaches to explore functional details.

The largest enzyme of respiratory chain complex I (or NADH:ubiquinone oxidoreductase) is a reversible redox-driven proton pump that has intrigued the bioenergetics community since the original studies from Sazanov's group unambiguously showed that all redox centers of the enzyme are located outside the membrane domain⁵. Therefore, in contrast to other proton-pumping respiratory complexes, the redox centers

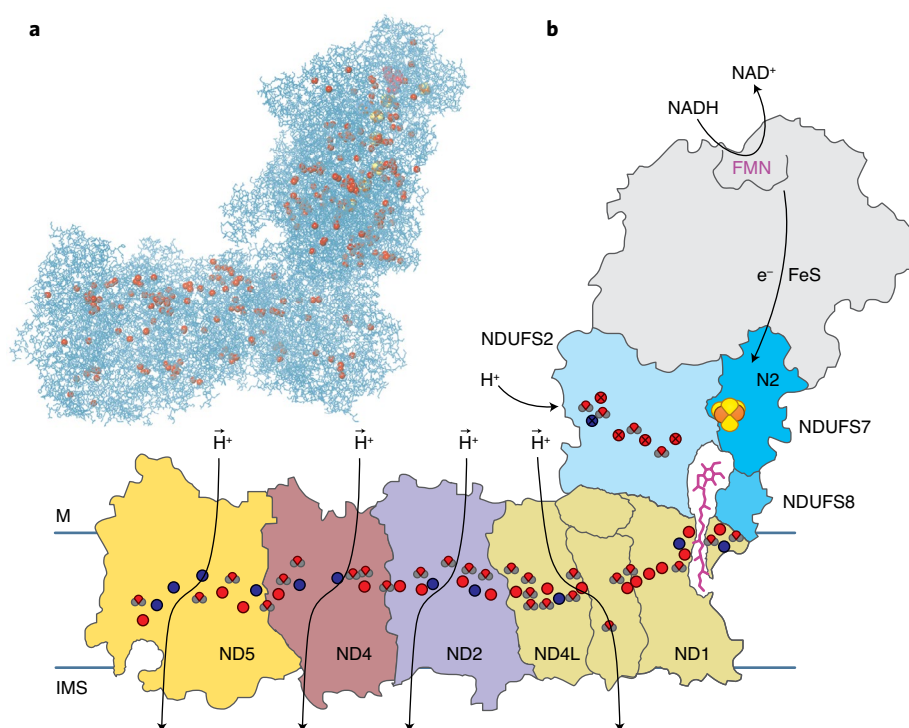


Fig. 1 | The *Yarrowia lipolytica* complex I structure determined by Grba and Hirst (PDB 6YJ4). a,

Overview of the structure, with protein chains shown as wires and water molecules as red spheres. FMN (magenta) and Fe-S clusters (orange and yellow) are also shown. **b,** Schematic diagram of respiratory complex I. Top right, the electron transfer direction, going from NADH via FMN and Fe-S clusters toward the ubiquinone molecule (magenta sticks); only the last Fe-S cluster (N2, orange and yellow) is shown, in the cavity formed by subunits NDUFS2, NDUFS7, NDUFS8 (blue) and ND1 (wheat). A chain of polar and charged residues (crossed red and blue circles) with water molecules (red and grey dipoles) in the NDUFS2 subunit (light blue) provides stoichiometric protons (H^+) for the ubiquinone reduction. The E-channel in ND1 connects the site of ubiquinone reduction to the first putative proton pump, organized by ND1, ND3, ND6 and ND4L (wheat). The central hydrophilic axis of polar and charged residues (red and blue circles) with water molecules is schematically shown. Ubiquinone reduction/binding in the cavity affects the protonation state of those key amino acid residues, resulting in proton exchange via formation and dissipation of water wires. Three antiporter-like subunits, ND2 (purple), ND4 (red) and ND5 (yellow) form three proton pumps connecting the matrix side (M) and the intermembrane space (IMS).

of complex I cannot participate directly in proton translocation. Three-dimensional structures of complex I from different species have since become available, but it

is still not clear how energy released during the redox reaction is transduced to drive proton pumping in the membrane domain.

The *Y. lipolytica* mitochondrial complex I comprises 14 core and 29 accessory subunits; its structure was first determined by X-ray crystallography^{6,7}, and it has also been determined more recently by cryo-EM⁸. The catalytic core subunits are remarkably similar in the bacterial and eukaryotic enzymes. NADH is oxidized at the hydrophilic top (Fig. 1b), and electrons are transferred downstream via the flavin mononucleotide (FMN) and a chain of iron-sulfur clusters to ubiquinone. The terminal Fe-S cluster (N2) that reduces ubiquinone is located ~30 Å above the membrane plane, so the ubiquinone head group that enters from the membrane is deeply embedded in the protein⁷ (Fig. 1b). The redox energy released during the sequential reduction of ubiquinone drives proton translocation, most likely via a cascade of conformational changes in four consecutively organized proton pumps. The so-called E-channel⁹ is probably the site of the initial step of vectorial proton translocation by the putative first pump, which is composed of subunits ND1, ND6 and ND4L. Energy is then transferred over a distance of around 150 Å to the distal membrane part, where the three largest antiporter-like core subunits (ND2, ND4 and ND5) form three successive proton pumps. A network of conserved charged and polar residues located around flexible breaks in transmembrane helices (π -bulges) forms the central hydrophilic axis in these core membrane subunits. Electrostatic interactions between neighboring domains connect the site of ubiquinone reduction (NDUFS2–NDUFS7–NDUFS8–ND1) and the E-channel with four proton pumps (Fig. 1b).

The new structure reveals a number of ordered water molecules bound to distinct functional modules of complex I, some of which were predicted in the bacterial enzyme^{10–12}. Stoichiometric protons (H⁺) needed for ubiquinone reduction are supplied from the mitochondrial matrix side via a relay pathway composed of at least four ordered water molecules located near charged residues of the NDUFS2 (49 kDa) subunit. The proton-pumping route in the membrane domain commences from three water molecules located at the top and two at the bottom of the E-channel at the ND1 subunit. Changes in electrostatic interactions after ubiquinone reduction probably affect the protonation state of the key amino acid residues, resulting in proton exchange during concerted transformation of water wires. In the first pump, the cavity formed by ND1 may contain unresolved water molecules that supply the first vectorial proton to conserved glutamate residues of ND1 and then to ND6. One

water molecule is located in the ND3–ND6–ND4L interface of the proposed proton exit pathway on the intermembrane space side.

The next chain of 20 ordered water molecules extends from the ND4L to ND5 subunits, hydrating the central axis. In addition, there are groups of water molecules on the matrix side of the proton-pumping ND2, ND4 and ND5 antiporter-like subunits, which are probably essential for the entrance of protons into the pumps. The formation of water chains in those entrance regions is probably sensitive to the protonation states of conserved residues within the hydrophilic central axis. Most likely, the dissociation and attachment of water molecules at hydrophilic entrances, induced by conformational rearrangements of ND2, ND4 and ND5, governs vectorial proton motions during enzyme turnover (Fig. 1b).

Energy propagates via the central hydrophilic polar axis and drives proton translocation through the four pumps by changing the conformation of transmembrane helices containing flexible π -bulges. Five vertical, well-conserved π -bulges stabilized by interactions with water molecules or polar groups were identified in the proton pumps ND1+ND6, ND2, ND4 and ND5^{9,10,13}. As suggested previously^{10,12}, the accessibility of internal polar residues at the proton entry sites on the matrix side may be governed by rotation of a conserved Leu-His gating pair found in antiporter-like subunits. Intriguingly, in the new structure, the putative gate is closed in ND5 and ND4 but open in ND2. In previous structures of bacterial⁹ and mammalian¹³ enzymes, all three gates were closed, indicating a species-specific feature in the *Y. lipolytica* enzyme or a new intermediate state in the catalytic cycle.

To drive proton pumping, the energy released during ubiquinone reduction should be converted into conformational changes in the core subunits. Different conceptual schemes have been proposed^{9,10,14–17}, but a comprehensive picture is elusive. Binding, reduction and release of the ubiquinone molecule is a multistep process, and it is unclear at which step energy is used to rearrange the polypeptides surrounding ubiquinone and how that is converted into conformational changes in the proton-translocating subunits. We still do not know the order of events occurring between ubiquinone reduction and priming of the first proton pump during catalytic turnover. Each pump could operate individually and propagate the energy to the neighboring subunit, driving the next pumping event. Alternatively, in one 'stroke', matrix protons

could bind to all four pumps and then, during the 'backstroke', conformational changes could cause all four protons to be released on the other side (loading–release scheme). The routes for proton exit are still under discussion, and the role of the newly observed small hydrophilic cavity at the end of the distal ND5 subunit (Fig. 1b) will require further investigation. Removal of the ND5 and ND4 subunits from *Y. lipolytica* complex I¹⁷ results in a functional enzyme with only two operational proton pumps, indicating that the function of the ND2 and ND1–ND6–ND4L machinery is independent of the presence of distal pumps, so it is possible that the pumps are organized in modules. Such an arrangement would be inconsistent with the recently proposed hypothesis of forward and reverse electrostatic waves¹⁶, thus further investigation is required to fully support this scheme.

Another crucial aspect of mitochondrial complex I operation is the A/D transition^{2,3}. Under ischemic conditions, when respiration is halted, the idle enzyme spontaneously converts to a deactive or resting state that can be activated by a slow turnover^{3,18}. This process involves substantial changes in the conformation and the exposure of several subunits close to the ubiquinone-binding site^{15,18}. The new structure clearly reveals the exact molecular basis for the functional differences between the two forms. The deactivating conformational changes involve the formation of a π -bulge in transmembrane helix (TMH) 3 of ND6, bending of TMH4 of ND1 and movement of the matrix-facing interhelical loops of ND1, ND3 and the β 1– β 2 loop of NDUFS2 to the outside. These changes affect the ND1 internal cavity, opening access from the matrix side and dramatically increasing its volume and extending the hydration of its surface. The new structure contains a bound DDM detergent molecule that might maintain the enzyme in the deactive state, which may be related to the fatty-acid-facilitated deactivation of the bovine enzyme¹⁹. The study by Grba and Hirst unequivocally shows that, following deactivation, exposure of the ND3 interhelical loop, which contains Cys40 (Cys39 in mammals), results from a motion of the loop itself, and not from a rearrangement of the surrounding subunits that insulate this region from the outside in the active form. Interestingly, covalent modification of this cysteine residue by a non-bulky NO group during nitrosation^{3,4} prevents enzyme activation, indicating the internal cavity of ND1 must be tightly sealed for ubiquinone reduction and binding. It would be tempting to search for a natural

matrix factor that targets the loops opening the ND1 cavity and therefore regulates the A/D transition in situ. A key question regarding the A/D transition is whether the D-form is an off-pathway state or an intermediate of the catalytic turnover of complex I; to answer this question, detergent-free and substrate-bound structures are required. □

Alexander Galkin  

Department of Pediatrics, Columbia University, New York, NY, USA.

✉e-mail: ag4003@cumc.columbia.edu

Published online: 21 August 2020

<https://doi.org/10.1038/s41594-020-0500-y>

References

1. Griba, D. & Hirst, J. *Nat. Struct. Mol. Biol.* <https://doi.org/10.1038/s41594-020-0473-x> (2020).
2. Kotlyar, A. B. & Vinogradov, A. D. *Biochim. Biophys. Acta* **1019**, 151–158 (1990).
3. Dröse, S., Stepanova, A. & Galkin, A. *Biochim. Biophys. Acta* **1857**, 946–957 (2016).
4. Chouchani, E. T. et al. *Nat. Med.* **19**, 753–759 (2013).
5. Sazanov, L. A. & Hinchliffe, P. *Science* **311**, 1430–1436 (2006).
6. Zickermann, V. et al. *Science* **347**, 44–49 (2015).
7. Hunte, C., Zickermann, V. & Brandt, U. *Science* **329**, 448–451 (2010).
8. Parey, K. et al. *Elife* **7**, e39213 (2018).
9. Baradaran, R., Berrisford, J. M., Minhas, G. S. & Sazanov, L. A. *Nature* **494**, 443–448 (2013).
10. Efremov, R. G. & Sazanov, L. A. *Nature* **476**, 414–420 (2011).
11. Haapanen, O. & Sharma, V. *Sci. Rep.* **7**, 7747 (2017).
12. Di Luca, A., Gamiz-Hernandez, A. P. & Kaila, V. R. I. *Proc. Natl Acad. Sci. USA* **114**, E6314–E6321 (2017).
13. Agip, A.-N. A. et al. *Nat. Struct. Mol. Biol.* **25**, 548–556 (2018).
14. Brandt, U. *Biochim. Biophys. Acta* **1807**, 1364–1369 (2011).
15. Verkhovskaya, M. L., Belevich, N., Euro, L., Wikström, M. & Verkhovskiy, M. I. *Proc. Natl Acad. Sci. USA* **105**, 3763–3767 (2008).
16. Kaila, V. R. I. *J. R. Soc. Interface* **15**, 20170916 (2018).
17. Dröse, S. et al. *PLoS Biol.* **9**, e1001128 (2011).
18. Babot, M., Birch, A., Labarbuta, P. & Galkin, A. *Biochim. Biophys. Acta* **1837**, 1083–1092 (2014).
19. Loskovich, M. V., Grivennikova, V. G., Cecchini, G. & Vinogradov, A. D. *Biochem. J.* **387**, 677–683 (2005).

Competing interests

The author declares no competing interests.